# Impact of Valley-Polarization on the Resistivity in Two-Dimensions

K. Takashina,[1] Y. Niida,[2] V.T. Renard,[3] A. Fujiwara,[4] T. Fujisawa,[5] K. Muraki,[4] and Y. Hirayama[2]

[1]*Department of Physics, University of Bath, Bath BA2 7AY, UK*
[2]*Graduate School of Science, Tohoku University,*
*6-3 Aramakiaza Aoba, Aobaku, Sendai, 980-8578 Japan*
[3]*Institut Néel, CNRS et Université Joseph Fourier, BP 166, F-38042 Grenoble Cedex 9, France*
[4]*NTT Basic Research Laboratories, NTT Corporation, Atsugi-shi, Kanagawa 243-0198, Japan*
[5]*Tokyo Institute of Technology, 2-12-1 Ookayama, Meguro-ku, Tokyo 152-8551, Japan*
(Dated: April 6, 2011)

We examine the temperature dependence of resistivity in a two-dimensional electron system formed in a silicon-on-insulator quantum well. The device allows us to tune the valley splitting continuously in addition to the electron density. Our data provide a global picture of how the resistivity and its temperature dependence change with valley polarization. At the boundary between valley-polarized and partially-polarized regions, we demonstrate that there is an insulating contribution from spin-degenerate electrons occupying the upper valley-subband edge.

PACS numbers: 71.30.+h, 72.20.-i, 72.10.Fk, 73.21.Fg, 73.40.Qv

Spin is crucial in determining the nature of the two dimensional electron system (2DES). Lifting spin-degeneracy by applying an in-plane magnetic field first dramatically increases the resistivity and second, tends to drive a metallic system into an insulating one [1–3]. Experiments had suggested that this is the case regardless of valley degeneracy, being observed in valley degenerate systems such as Si-MOSFETs [3, 4] as well as non-valley-degenerate p-type GaAs [5]. The detailed phenomenology is, however, more complex [6–11] and has yet to be fully understood. It might be expected that the role played by the valley degree of freedom is, in essence, equivalent to that of the spin degree of freedom since interactions between electrons are mediated by the Coulomb interaction. This, to some extent, has been demonstrated in recent experiments in AlAs quantum wells [12] in which a valley splitting is induced and tuned by applying symmetry breaking strain. These experiments showed that for certain fixed electron densities, spin and valley both need to be polarized before insulating behavior is observed in contrast to previous experiments in silicon where lifting only the spin degeneracy is sufficient to induce a transition to insulating behavior. This indicates that other parameters must also be at play. Electron density and disorder are both already known to be vital and call for these to be examined in conjunction with spin and valley degrees of freedom.

In this Letter, we address the temperature dependence of the resistivity in silicon-on-insulator quantum-well structures in which the valley-splitting can be swept electrically, in addition to, and independently from the electron density [13]. We find that increasing valley polarization increases resistivity, and strong metallic temperature dependence is suppressed, although incompletely, depending on density. Furthermore, upon crossing the valley partially-polarized-fully-polarized boundary, our data reveal an insulating contribution to the resistivity arising from the upper-valley-subband edge. We hypothesize that this may be due to scattering induced by localized magnetic moments [14] in the localized tail of the upper valley subband via a Kondo mechanism [15]. In turn, our results suggest that in parallel magnetic field experiments of valley-degenerate systems, localized valley-moments may scatter electrons in the lower spin subband via an analogous mechanism which may provide an avenue for understanding some of the unexplained phenomenology.

The quantum well [Fig.1] consists of a monocrystalline layer of nominally 10 nm thick silicon with front- and back-gate oxide thicknesses of 75 nm and 380 nm respectively. A standard four-terminal lock-in technique was used to measure the resistivity $\rho$ of a sample with a Hall-bar geometry. Electron density as function of front- and back-gate voltages $V_{\mathrm{F}}$ and $V_{\mathrm{B}}$ was calibrated from Hall effect measurements and Shubnikov de Haas oscillations, the latter also providing the valley-splitting $\Delta_{\mathrm{V}}$ as previously described in detail [13]. The total electron density $n$ can be approximated by a simple capacitor model: $n = n_{\mathrm{F}} + n_{\mathrm{B}} = (C_{\mathrm{F}}(V_{\mathrm{F}} - V_{\mathrm{F}}^{\mathrm{Th}}) + C_{\mathrm{B}}(V_{\mathrm{B}} - V_{\mathrm{B}}^{\mathrm{Th}}))/e$ where $n_{\mathrm{F}}$ and $n_{\mathrm{B}}$ are electron densities contributed by front and back gates with capacitances $C_{\mathrm{F}} = 462\ \mu\mathrm{Fm}^{-2}$ and $C_{\mathrm{B}} = 88\ \mu\mathrm{Fm}^{-2}$ respectively and $V_{\mathrm{F}}^{\mathrm{Th}}$ and $V_{\mathrm{B}}^{\mathrm{Th}}$ are constant offsets. The valley splitting is approximated by a phenomenological formula: $\Delta_{\mathrm{V}} = \alpha\delta n$ when $\delta n > 0\ \mathrm{m}^{-2}$ where $\delta n = n_{\mathrm{B}} - n_{\mathrm{F}}$ reflects the out-of-plane electrostatic asymmetry [Fig. 1(d)]. The valley factor $\alpha$ for the Si-buried oxide interface in this sample has a value of about $0.49\ \mathrm{meV}/10^{15}\ \mathrm{m}^{-2}$.

The resistivity measured at a temperature of 350 mK is presented in figure 2(a). According to the simple capacitor model, there is a one-to-one mapping between $(V_{\mathrm{B}}, V_{\mathrm{F}})$ which we sweep in the experiment and $(\delta n, n)$, axes for which are marked on the figure [16]. When $\delta n = 0\ \mathrm{m}^{-2}$, the quantum well is biased symmetrically

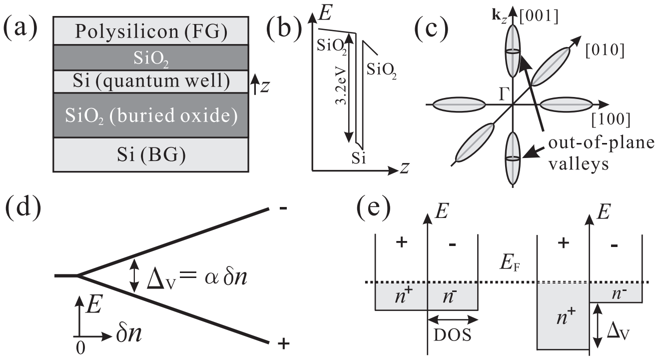


FIG. 1: (a) Schematic sample structure. (b) Schematic band lineup. (c)Fermi surfaces of electrons in bulk silicon. Only out-of-plane valleys are occupied in our device. (d) Electrostatic bias $\delta n$ increases valley splitting between coupled out-of-plane valleys + and -. (e) Resulting density of states without (*left*) and with (*right*) valley splitting.

about its centre. As usual, resistivity is divergent at very low $n$ and decreases with increasing $n$ until the antisymmetric upper confinement subband starts to fill. The estimated onset of upper subband occupation is marked by a dotted line and $\rho$ is enhanced along it.

When $\delta n$ is increased, the electrostatic symmetry of the quantum well is broken, and the wavefunction in the confinement direction shifts towards the buried-oxide. This is accompanied by increased valley splitting, leading to a region of valley polarization bound by the lines of zero density and the onset of occupation of the upper valley subband highlighted by a dashed line in the figure. The data clearly show that the resistivity is enhanced in this region. The same data is plotted in figure 2(c) (solid lines) as a function of $\delta n$ which scales linearly with the valley splitting, at various values of density $n$. In all these traces, resistivity increases as full valley polarization is approached accompanied by a shoulder demarcating the onset of full valley polarization. The appearance is remarkably similar to previous reports in which an in-plane magnetic field is applied to polarize spin (instead of valley) [3–5, 8], leading to a saturation of $\rho$ when full spin polarization is reached. Our results, therefore, lend strong support to the equivalence of valley and spin [12]. In our case, increasing $\delta n$ has another effect of pressing the out-of-plane wavefunction against the silicon-silicon dioxide interface, increasing the effects of interface roughness, leading to resistivity which continues to increase with $\delta n$. The resistivity increase towards $\delta n = 0$ m$^{-2}$ at high $n$ is due to the occupation of the upper confinement subband.

Data taken at a higher temperature of $T = 5$ K is also superimposed [short-dashed lines, Fig. 2(c)]. Clearly, the manner in which temperature dependence evolves is non-trivial showing changes in sign and magnitude as density and valley splitting are varied. In order to obtain an

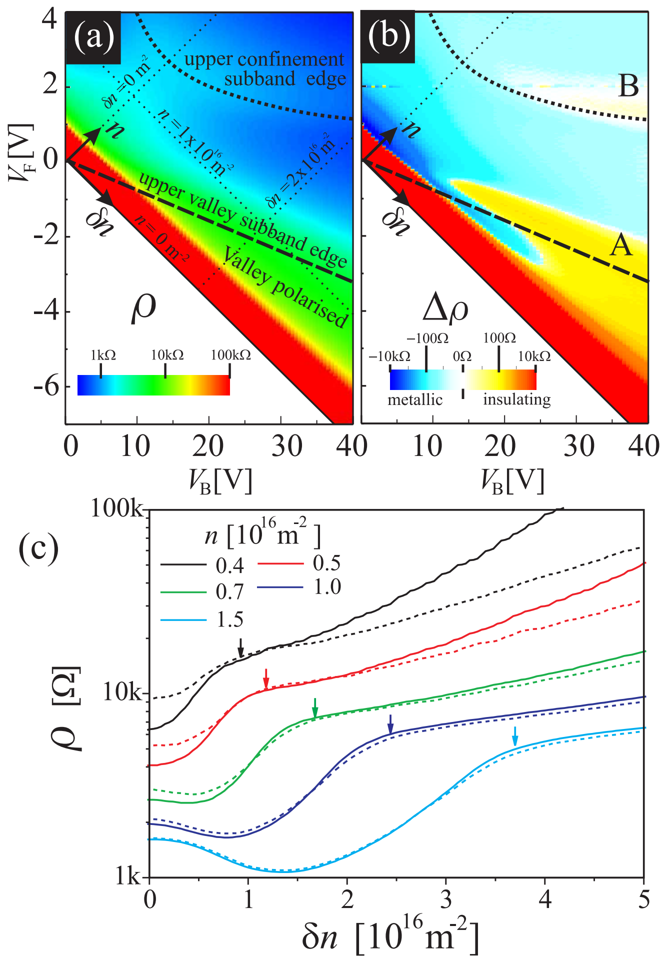


FIG. 2: Color online. (a) Color plot of $\rho$ at $T = 350$ mK. The thick dashed line marks the estimated boundary between partially and fully valley polarized regions. For $\rho > 100$ kΩ, the same color as $\rho = 100$ kΩ is used. (b) Change in resistivity between $T = 0.35$ K and $T = 5$ K: $\Delta\rho = \rho(T = 0.35\text{ K}) - \rho(T = 5\text{ K})$. For $\Delta\rho > 10$ kΩ and $\Delta\rho < -10$ kΩ, colors for $\Delta\rho = 10$ kΩ and $\Delta\rho = -10$ kΩ are used respectively. (c) Resistivity at various densities $n$ plotted as a function of $\delta n$. Arrows mark the calculated edge of the upper valley subband. Solid lines: 350 mK, dashed lines: 5 K.

overview of the temperature dependence on the $(V_B, V_F)$-plane, we present a color plot of the change in resistivity between 0.35 K and 5 K. i.e. $\Delta\rho = \rho(T = 0.35\text{K}) - \rho(T = 5\text{K})$ [Fig. 2(b)].

When $\delta n$ is small the valley splitting is small and the system is mildly metallic at high density. As the density is lowered it becomes more and more metallic until at very low density, the system undergoes a transition to an insulating state. As $\delta n$ is increased the valley splitting increases, and an interesting picture emerges where metallic behavior continues into the valley polarized region. At larger $\delta n$, however, only insulating temperature dependence is observed under valley polarization. As the out-of-plane electric field is increased, surface roughness induced disorder enhances localization which in turn causes strong insulating behavior to be extended to higher density. However, it is strikingly clear from the data that $\Delta\rho$ does not simply depend monotonically on density, out-of-plane bias and whether or not the system is valley polarized. The data show a clear additional insulating contribution (feature A [Fig. 2(b)]) near the valley-polarized - partially polarized boundary where the Fermi energy is near the upper valley subband edge (thick dashed line [Fig. 2(b)]). Insulating behavior is also seen (feature B [Fig. 2(b)]) near the onset of occupation of the upper confinement subband (thick dotted line [Fig. 2(b)]) suggesting that this effect is general to all types of subbands.

We hypothesize that this insulating contribution is due to electrons localized in the disorder broadened tail of the upper subband [Fig. 3(a)]. Since these localized electrons possess the spin degree of freedom, they can behave as magnetic impurities, i.e. local moments, and scatter electrons in the lower subband in analogy with the Kondo effect in metals [Fig. 3(b)][15]. Previous experiments by Feng et al. on conventional silicon MOSFETs provided evidence that such localized electrons do indeed enhance resistivity and that their presence acts to destroy metallic temperature dependence [14]. For such a scattering process to be effective, localized states must be singly occupied, lying sufficiently close to the Fermi level. Thus one would expect that taking the Fermi energy well above the localized tail into the extended states of the upper subband would quench this scattering process. However, previous studies have been limited to conditions where the Fermi energy lies far below the mobility edge of the upper subband [14].

In the present experiment, we can readily tune the Fermi level through the edge of the upper subband: As $V_{\mathrm{F}}$ is increased and swept through feature A [Fig. 2(b)], the number of localized electrons first increases, and their effect on the resistivity increases. With density increased further, the Fermi level moves further above these localized states and localized electrons may pair up to form singlets quenching their spin angular momentum. Concurrently, the localization length of states at the Fermi energy increases and their corresponding on-site Coulomb energy decrease until delocalized states are reached where further upper subband electrons can no longer scatter in this way. The resulting effect is an insulating contribution which, on the $V_{\mathrm{B}}$,$V_{\mathrm{F}}$-plane, lies specifically where the Fermi energy is close to an upper valley subband edge.

Evidence for the involvement of spin is provided by measurements under in-plane magnetic field. The change in resistivity $\Delta\rho^{B_\parallel} = \rho(B_\parallel = 15\ \mathrm{T}) - \rho(B_\parallel = 0\ \mathrm{T})$ is plotted in figure 3(c). Since the changes with field are relatively small at the features of interest, on a background with strong density and temperature dependence, detailed measurements were also made at a fixed back-gate voltage of $V_{\mathrm{B}} = 40$ V, sweeping $V_{\mathrm{F}}$ at consecutive values

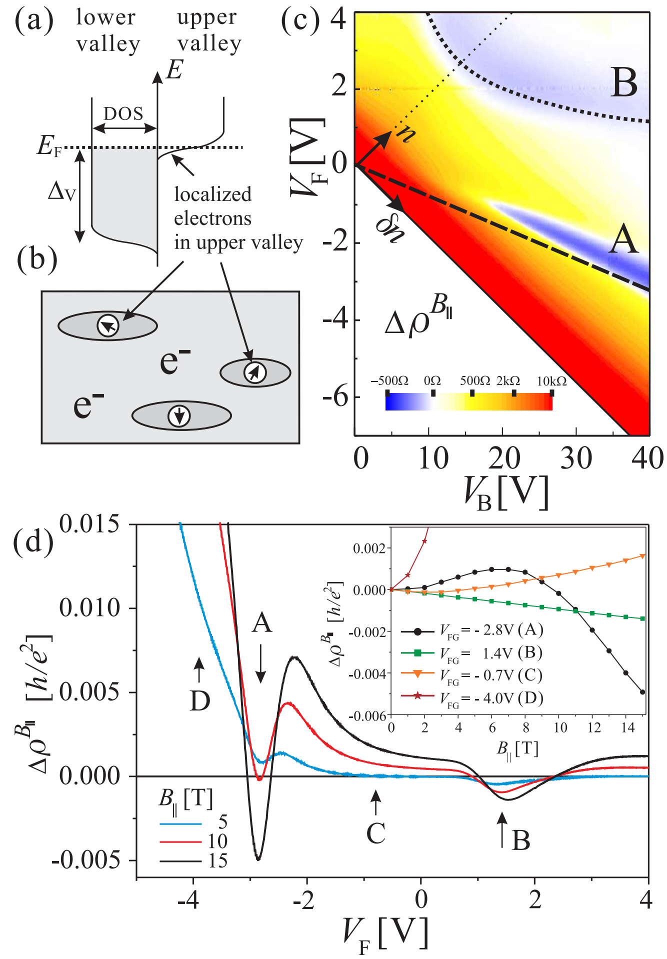


FIG. 3: Color online. (a) Schematic diagram of the density of states with disorder-broadened subband tails. (b) Plane view schematic. Electrons localized in the disorder broadened tail of the upper valley subband behave as magnetic impurities, leading to additional scattering for electrons in the lower subband. (c)Change in the resistivity between $B_\parallel = 15$ T and $B_\parallel = 0$ T: $\Delta\rho^{B_\parallel} = \rho(B_\parallel = 15\ \mathrm{T}) - \rho(B_\parallel = 0\ \mathrm{T})$. $T = 1.5$ K. For $\Delta\rho^{B_\parallel} > 10$ k$\Omega$, the same color as $\Delta\rho^{B_\parallel} = 10$ k$\Omega$ is used. (d) $\Delta\rho^{B_\parallel}$ at $V_{\mathrm{B}} = 40$ V at various values of $B_\parallel$. *Inset*: $\Delta\rho^{B_\parallel}$ as a function of $B_\parallel$ at A, B, C and D as marked in the main figure.

of magnetic field $B$ [17]. Results are presented in Fig 3 (d). The data clearly show that there is a background of positive magnetoresistance, and specifically where we find this additional insulating contribution (feature A), the system exhibits negative magnetoresistance.

If we suppose that the upper and lower subbands contribute conductance independently and that there are no inter-subband interactions, there should only be positive magnetoresistance, since the lowest subband only shows positive magnetoresistance. Our results therefore strongly suggest that the resistivity of the lower subband is enhanced due to the occupation of the upper subband edge at zero magnetic field, and that this enhancement weakens with increased magnetic field.

Orbital effects [18] are highly unlikely to be responsible. The upper and lower valley subbands occupy the same confinement state which determines the out-of-plane envelope wavefunction. Furthermore, these valley states are known not to couple with in-plane magnetic field [19], leaving the spin as the remaining culprit. As the magnetic field is increased, the localized electrons in the upper subband spin polarize and can no longer scatter via their spin [20].

The magnetic field dependence $\Delta\rho^{B_\parallel}$ at A is plotted in the inset of Fig. 3(d). At low field, there is first a positive magnetoresistance followed by a maximum and then a negative magnetoresistance. This points to a competition between a positive magnetoresistance due to the lower subband, as also seen outside the region in $V_{\rm F}$ showing feature A (such as at C and D), and a negative contribution due to localized spins. The positive magnetoresistance of a single-subband system is generally interpreted as being due to the spin polarization of the 2DES [2, 21]. At the upper valley subband edge at $V_{\rm B} = 40$ V, the magnetic field required to fully polarize electrons in the lower subband is of order 250 T, and 15T used in the present experiment is relatively modest. Positive magnetoresistance becomes weaker with increased density since the polarization becomes smaller for a given magnetic field. Indeed, this accounts for our result that the net negative magnetoresistance of feature A disappears in Fig. 3(c) at lower $V_{\rm B}$ as the valley subband edge shifts to lower density $n$. We point out that at much higher density, negative magnetoresistance is also observed for the upper confinement subband (feature B). Although orbital effects cannot be ruled out in this case, since the electron density is greater, the background positive magnetoresistance is weaker and the net magnetoresistance is negative even at 1T.

Finally, returning our attention to the equivalence of spin and valley degrees of freedom, our findings suggest that an analogous effect should be present in in-plane field experiments of valley degenerate systems [8–11]. In these spin-polarization experiments, electrons localized in the upper spin subband would be able to scatter electrons in the lower spin subband by virtue of their possessing the valley degree of freedom, i.e. by a valley-Kondo effect as predicted and experimental evidence for which has been reported for silicon quantum dots [22]. Mapping our phenomenology to the spin-polarization experiments, these localized valley-moments will contribute insulating temperature dependence to resistivity precisely when $E_{\rm F}$ lies close to the upper spin subband edge, whose magnitude will depend on the valley splitting. Si/SiGe, known to have much smaller $\Delta_{\rm V}$ [23] compared to Si MOSFETs, would show the strongest manifestation of this effect. Indeed, experiments on a Si/SiGe high mobility 2DEG by Lai et al. [8] find that for certain densities, there is a clear re-entrant temperature dependence where insulating temperature dependence is observed around the shoulder in resistivity at the onset of spin polarization. On the other hand, in standard Si MOSFETs with greater valley splitting, this re-entrant temperature dependence effect is found to be weaker [9] or masked by other mechanisms such as weak localization [11].

In conclusion, we confirm that valley polarization leads to enhanced resistivity in a similar manner as in-plane magnetic field in previous experiments. Furthermore, we have demonstrated that there is an additional insulating contribution from spin-degenerate electrons occupying the upper valley-subband edge, at the boundary between fully and partially valley-polarized regions. Clearly, further work is required to determine the detailed physics of this phenomenon, and importantly, how this extrapolates to low densities pertaining to the so-called metal insulator transition.

VTR acknowledges the support from Nanoscience Foundation and YH acknowledges support from JST programs.


[1] B. Spivak, S.V. Kravchenko, S.A. Kivelson and X.P.A. Gao, Rev. Mod. Phys. **82**, 1743 (2010)

[2] S.V. Kravchenko and M.P. Sarachik, Rep. Prog. Phys. **67**, 1 (2004)

[3] A. Prinz, V.M. Pudalov, G. Brunthaler and G. Bauer, Supperlatices and Microstructures, **27** 301 (2000)

[4] T. Okamoto, K. Hosoya, S. Kawaji and A. Yagi, Phys. Rev. Lett., **82**, 3875 (1999)

[5] E. Tutuc, E.P. De Poortere, S.J. Papadakis and M. Shayegan, Phys. Rev. Lett., **86**, 2858 (2001)

[6] A.A. Shashkin, S.V. Kravchenko and T.M. Klapwijk, Phys. Rev. Lett., **87**, 266402 (2001)

[7] K. Eng, X.G. Feng, D. Popović and S. Washburn, Phys. Rev. Lett., **88** 136402 (2002)

[8] K. Lai, W. Pan, D.C. Tsui, S.A. Lyon, M. Mühlberger and F. Schäffler, Phys. Rev. B., **72**, 081313(R) (2005)

[9] A.A. Shashkin, E.V. Deviatov, V.T. Dolgopolov, A.A. Kapustin, S. Anissimova, A. Venkatesan, S.V. Kravchenko and T.M. Klapwijk, Phys. Rev. B, **73**, 115420 (2006)

[10] K.M. Mertes, H. Zheng, S.A. Vitkalov, M.P. Sarachik and T.M. Klapwijk, Phys. Rev. B, **63**, 041101(R) (2001)

[11] A. Lewalle, M. Pepper, C.J.B. Ford, D.J. Paul and G. Redmond, *Phys. Rev. B*, **69**, 075316 (2004)

[12] O. Gunawan, T. Gokmen, K. Vakili, M. Padamanabhan, E.P. De Poortere and M. Shayegan, Nature Physics, **3** 388 (2007)

[13] K. Takashina, Y. Ono, A. Fujiwara, Y. Takahashi, Y. Hirayama, Phys. Rev. Lett., **96**, 236801 (2006)

[14] X.G. Feng, Dragana Popovic and S. Washburn, *Phys. Rev. Lett.* **83**, 368 (1999)

[15] J. Kondo, Prog. Theoret. Phys. **32**, 37 (1964)

[16] The lines marking the region of valley polarization and zero density are calculated using the simple capacitor model and parameters quoted. These were obtained by a best fit to data extending over the entire $(V_{\rm B}, V_{\rm F})$ range shown in the color plots. The lines are intended to provide

a guide, but are not of sufficient accuracy for analysing quantitative aspects of the metal-insulator-transition at low density.

[17] We have made similar measurements on 3 samples from two different wafers. All samples showed qualitatively the same behavior.

[18] J.A. Simmons, S.K. Lyo, N.E. Harff and J.F Klem, Phys. Rev. Lett., **73**, 2256 (1994), O.E. Raichev and F.T. Vasko, *Phys. Rev. B*, **53**, 1522 (1996)

[19] M.A. Wilde *et al.*, *Phys. Rev. B*, **72**, 165429 (2005)

[20] T.A. Costi, Phys. Rev. Lett., **85**, 1504 (2000), S. Foner, J. Appl. Phys., **40**, 1470 (1969)

[21] V.T. Dolgopolov and A. Gold, JETP Lett., **71**, 27 (2000)

[22] G.P. Lansbergen, G.C. Tettamanzi, J. Verduijn, N. Collaert, S. Biesemans, M. Blaauboer and S. Rogge, Nanoletters, **10**, 455 (2010), S.Y. Shiau, S. Chutia and R. Joynt, Phys. Rev. B, **75**, 195345 (2007)

[23] S. Goswami, K.A. Slinker, M. Friesen, L.M. McGuire, J.L. Truitt, C. Tahan, L.J. Klein, J.O. Chu, P.M. Mooney, D.W. van der Weide, Nature Physics, **3**, 41 (2007)